HHS Public Access

Author manuscript

FEBS Lett. Author manuscript; available in PMC 2016 February 04.

Published in final edited form as:

FEBS Lett. 2015 July 8; 589(15): 1904–1910. doi:10.1016/j.febslet.2015.05.047.

Altered epidermal lipid processing and calcium distribution in the KID syndrome mouse model Cx26S17F

Felicitas Bosen[a], **Anna Celli**[b], **Debra Crumrine**[b], **Katharina vom Dorp**[c], **Philipp Ebel**[a], **Holger Jastrow**[d], **Peter Dörmann**[c], **Elke Winterhager**[d], **Theodora Mauro**[b], and **Klaus Willecke**[a,*]

[a]LIMES (Life and Medical Science Institute), Molecular Genetics, University of Bonn, 53115 Bonn, Germany

[b]Department of Dermatology, SF-VAMC and UCSF, San Francisco, CA, USA

[c]Institute of Molecular Physiology and Biotechnology of Plants, University of Bonn, Germany

[d]Electron Microscopy Unit, Imaging Center Essen, University Clinic Essen, Germany

Abstract

The keratitis–ichthyosis–deafness (KID) syndrome is caused by mutations in the gap junctional channel protein connexin 26 (Cx26), among them the mutation Cx26S17F. Heterozygous Cx26S17F mice resemble the human KID syndrome, i.e. exhibiting epidermal hyperplasia and hearing impairments. Newborn Cx26S17F mice show a defective epidermal water barrier as well as altered epidermal lipid secretion and location. Linoleoyl ω-esterified ceramides are strongly decreased on the skin surface of Cx26S17F mice. Moreover, the epidermal calcium gradient is altered in the mutant mice. These alterations may be caused by an abnormal Cx26S17F channel function that leads to a defective epidermal water barrier, which in turn may trigger the hyperproliferation seen in the KID syndrome.

Keywords

Keratitis–ichthyosis–deafness syndrome; Connexin 26; Transgenic mouse mutant; Epidermal water barrier defect; Epidermal calcium gradient; Epidermal ceramides

1. Introduction

The keratitis–ichthyosis-deafness (KID) syndrome (OMIM #148210) is a rare autosomal-dominant hereditary disease, affecting the skin, the cochlea and the eyes of patients. Skin defects in the KID syndrome include thickening of all epidermal layers, palmoplantar

*Corresponding author at: LIMES Institute, Molecular Genetics, University of Bonn, Carl-Troll-Straße 31, 53115 Bonn, Germany. Fax: +49 2287362642. k.willecke@uni-bonn.de (K. Willecke)..

Author contributions: KW and FB conceived and designed the study; FB, AC, DC, KvD, PE and HJ acquired the data; KW, PD, EW, and TM supervised the study; FB and KW drafted the manuscript; FB, AC, DC, KvD, PE, HJ, PD, EW, TM and KW analyzed data and made critical manuscript revisions.

Conflict of interest The authors declare no conflict of interest.

Appendix A. Supplementary data Supplementary data associated with this article can be found, in the online version, at http://dx.doi.org/10.1016/j.febslet.2015.05.047.

hyperkeratosis and hyperkeratotic plaques. Moreover, KID patients suffer from prelingual sensorineural hearing loss (SNHL) and chronic inflammation of the eye's cornea [1].

The main function of the multilayered epidermis is to maintain a barrier which prevents water, bacteria and toxin penetration as well as water loss from the body. This epidermal barrier is mainly established by the cornified envelope and the extracellular lipid lamellae of the stratum corneum [2]. Besides free fatty acids, cholesterol and cholesterol esters, the main component of the extracellular lipid lamellae of the stratum corneum are ceramides, which show a large diversity in their acyl residues as well as in the degree of saturation of their long chain base residues [3,4]. These ceramides are synthesized during epidermal differentiation in the stratum granulosum and packed into membrane enclosed lamellar bodies. After secretion at the interface between stratum granulosum and stratum corneum they surround the corneocytes of the stratum corneum, constituting the major portion of the extracellular lipid lamellae.

An epidermal calcium gradient is known to regulate the epidermal differentiation as well as lipid secretion and is therefore a prerequisite for an intact epidermal barrier [5]. In healthy skin there is a relatively low amount of calcium ions in the stratum basale. During differentiation the calcium concentration rises and peaks in the stratum granulosum. During the last differentiation step the calcium ions are removed intra- and extracellularly from the stratum corneum [6–8].

Connexins are the transmembrane protein subunits of gap junction channels which mediate the exchange of ions and small molecules up to a mass of 1.8kDa [9]. As members of a multigene family, 21 different connexin isoforms are known to be expressed in humans, while 20 connexin isoforms have been described in mice [10]. Six connexin subunits oligomerize to build a hexameric hemichannel, which can interact with a hemichannel of a contacting cell to form an intercellular gap junction channel [11]. Connexin hemichannels can be involved in paracrine and autocrine signaling by connecting the cytoplasm to the extracellular environment and facilitating the diffusional exchange of molecules and ions such as IP3, ATP and calcium [12].

Several mutations in the human Cx26 gene GJB2 have been associated with the KID syndrome. One of them leads to the exchange of a serine residue by a phenylalanine residue at position 17 of the Cx26 amino acid sequence (Cx26S17F), located near the N-terminus of the Cx26 protein [13]. Expression and dye transfer analyses of the mutated Cx26S17F protein in HeLa cells and Xenopus oocytes showed that the Cx26S17F protein can be transported to the plasma membrane but forms coupling deficient gap junction channels and inactive homotypic hemichannels [13,14]. However, a recent study suggests that if Cx26S17F is co-expressed with wild type Cx26 or Cx43 in transfected HeLa cells, the hemichannel activity is increased compared to homo-meric wild type hemichannels [15]. These results with heteromeric Cx26S17F/Cx26wt channels are more likely to represent the situation in patients suffering from the autosomal dominant KID syndrome.

Previously we have described the Cx26S17F mouse mutant which resembles the KID syndrome in many aspects. Heterozygous Cx26S17F+/flox: PGK-Cre mice (here referred to

as “Cx26S17F mice”) showed a dry, scaly skin. Adult Cx26S17F mice exhibited epidermal hyperproliferation and strong hyperplasia of all epidermal layers. Furthermore, the hearing of Cx26S17F mice was impaired [16].

In order to explain the skin phenotype of Cx26S17F mice and KID patients, here we have further characterized the epidermis of newborn Cx26S17F mice by analyzing the distribution, secretion and composition of epidermal lipids as well as of the distribution of the epidermal calcium gradient.

2. Materials and methods

2.1. Treatment of mice

All experiments were performed with littermates of >87.5% BL/6N genetic background.

All mice used in this study were kept under standard housing conditions with a 12 h/12 h dark–light cycle with food and water ad libitum. All experiments were carried out in agreement with local and state regulations for research with animals.

2.2. Generation/breeding of mice

The generation of the conditional Cx26S17F mouse was described in detail by Schütz et al. [16]. Female Cx26S17Fflox/flox mice were bred with male phosphoglycerate kinase (PGK)-Cre recombinase expressing mice leading to exchange of wild type Cx26 by Cx26S17F in every cell type endogenously expressing Cx26. In this study Cx26S17F+/flox mice are referred to as “control mice”, whereas Cx26S17F+/flox: PGK-Cre mice are referred to as “Cx26S17F mice”.

2.3. Nile red staining

For Nile Red stainings, paw cryosections were fixed in 4% paraformaldehyde, incubated for 2 h with 5 μg/mL Nile Red solution (Sigma–Aldrich, Cat. No. 72485, St. Louis, MO, USA) and mounted with Glycergel mounting medium (DakoCytomation, Glostrup, Denmark).

2.4. Electron microscopy and ion-capture cytochemistry

The skin biopsies were fixed in modified Karnovsky fixative (2% formaldehyde and 2% glutaraldehyde in 0.1 M cacodylate buffer, pH 7.2) and post-fixed in either 0.2% RuO_4 or 1% OsO_4 [17]. For ion-capture cytochemistry the samples were fixed in ice-cold fixative containing 2% glutaraldehyde, 2% formaldehyde, 90 mM potassium oxalate, and 1.4% sucrose (pH 7.4) in the dark for 1–2 h [6]. The samples were then postfixed in 1% OsO_4 containing 2% potassium pyroantimonate at 4 °C in the dark for 2 h. All samples were then dehydrated and embedded in Epoxy resin [6]. Ultrathin sections stained with 1% uranyl acetate and 0.4% lead citrate were examined in either a JEOL (Jeol Ltd., Japan) or in a Zeiss EM9-02 (Zeiss, Germany) transmission electron microscope.

2.5. Lipid extractions

For extraction of epidermal lipids, skin and paw skin was incubated with Dispase II (2 U/mL in PBS, Sigma–Aldrich, St. Louis, MO, USA) overnight at 4 °C. After washing with PBS

the epidermis could be separated from the dermis. The epidermis was homogenized in water using a Precellys tissue homogenizer (PEQLAB, Erlangen, Germany) and lyophilized. Epidermal lipids were extracted for 24 h at 37 °C in each of three solvent mixtures: chloroform/methanol/water 1:2:0.5 (v/v/v); chloroform/methanol 1:1 (v/v), and chloroform/methanol 2:1 (v/v). The final supernatant was used for mass spectrometry analyses.

Surface lipids were extracted using a protocol described previously [18], modified as follows: Newborn (P0) mice were sacrificed by inhalation of isoflurane. To release epidermal lipids whole mice were covered in *n*-hexane/ethanol 2:1 (v/v) for 10 min. The organic solvent was evaporated under a stream of nitrogen at 50 °C and lipids were extracted in chloroform/methanol/water 2:1:0.8 (v/v/v) followed by sonification for 5 min. Then chloroform and water were added to the final ratio of chloroform/methanol/water 2:2:1.8 (v/v/v), vortexed and centrifuged for phase separation. The lower lipid-containing chloroform phase was collected and evaporated under a stream of nitrogen.

2.6. Mass spectrometry analyses

Relative amounts of epidermal ceramides of Cx26S17F mice compared to wild type mice were quantified using the Agilent 6530 Accurate-Mass Q-TOF LC/MS instrument equipped with a direct infusion chip-based nanospray ion source. The nanospray solvent was chloroform/methanol/300 mm ammonium acetate (300:665:35) [19]. Sphingolipids were ionized in the positive mode. Instrumental parameters were set as described previously [20]. Cer[EOS], Cer[AS] and Cer[NS] were quantified using precursor ion scanning for a characteristic fragment, *m*/*z* 264.2686, generated after collision-induced dissociation and normalized to the internal standard d18:1–12:0 ceramide (Avanti Polar Lipids). Data are represented as mol% of total sphingolipids detected.

2.7. Immunoblot analyses

Total proteins were extracted from skin using a Precellys tissue homogenizer (PEQLAB, Erlangen, Germany) in lysis buffer (2 × Complete [Roche, Mannheim, Germany], 1% Triton X-100, 0.5% Nonidet P40, 50 mM NaCl, 30 mM $Na_4P_2O_7 \cdot 10 \times H_2O$, 1 mM Na_3VO_4, 50 mM NaF, 1 mM PMSF, 20 mM HEPES) 4 times for 20 s and centrifuged at 6800×*g*. Laemmli buffer [21] was added to protein lysates and 50 μg proteins were separated by electrophoresis in 12% sodium dodecyl sulfate polyacrylamide gels. Then the proteins were transferred to a Hybond ECL membrane (Amersham Biosciences, Buck, UK) and blocked with 5% milk powder in TBST (10 mM Tris, 150 mM NaCl, 0.1% Tween-20, pH 7.5) for 1 h at room temperature. The membranes were incubated with primary mouse anti-PCNA antibodies (diluted 1:250, Santa Cruz Biotechnology, Dallas, TX, USA; Cat. No. sc-25280) overnight at 4 °C. After incubation with primary antibodies the membranes were washed 3 times with TBST at room temperature and incubated for 1 h with horse-radish peroxidase-conjugated secondary antibodies (goat anti-mouse, diluted 1:10000, Jackson ImmunoResearch, West Grove, PA, USA). For detection the membranes were incubated with enhanced chemiluminescence reagents (Pierce, Rockford, IL, USA). Loading controls were performed with mouse anti-tubulin antibodies (diluted 1:20000, Sigma–Aldrich, St. Louis, MO, USA Cat. No. T9026).

2.8. Immunofluorescence analyses

For immunofluorescence analyses skin biopsies were frozen in Tissue-Tek embedding medium (Sakura, Zoeterwonde, Netherlands). 14 μm cryosections were fixed in 4% paraformaldehyde for 5 min, washed 3 times in TBS-TX (50 mM Tris, 1.5% NaCl, 0.3% TritonX-100) and blocked for 1 h with 4% bovine serum albumin and 1% normal goat serum in TBS-TX. Primary rat anti-Ki67 antibody (monoclonal, diluted 1:50, DakoCytomation, Glostrup Denmark, Cat. No. M7249) was diluted in blocking solution and incubated with cryosection over night at 4 °C. Afterwards the sections were washed 3 times with TBS-TX and incubated with secondary antibodies Alexa Fluor 546 goat anti-rat IgG (diluted 1:1000, Invitrogen, Cat. No. A-11081, USA) for 45 min. Then the stained sections were washed 3 times with TBS-TX, embedded in Glycergel mounting medium (DakoCytomation), and analyzed by confocal microscopy (Zeiss, LSM 710, Germany).

2.9. Statistical analyses

Two-tailed Student's *t*-tests were used for statistical analyses. A *P*-value of <0.05 was regarded as statistically significant. Asterisks indicate a *P*-value of <0.05 (*), <0.01 (**) or <0.001 (***). Error bars represent standard error of the mean (S.E.M.).

3. Results

3.1. Disarrangement of lipids in the stratum corneum

Previous analyses using toluidine blue staining on newborn Cx26S17F mice indicated a water barrier defect in the mutated mice [16]. Additional experiments with X-gal dye penetration revealed that the water barrier was disrupted already during late embryonic development on embryonic day 21.5 (data not shown).

To define the basis for the observed water barrier defect, the epidermal lipid distribution was analysed by lipid stainings of skin cryosections and by electron microscopy (EM) analyses. Staining with the fluorescent lipid dye Nile red on paw cryosections showed that in newborn and in adult Cx26S17F mice lipids accumulated in a dot-like pattern in the stratum corneum while in control mice the lipids were evenly distributed in extracellular lipid lamellae (Fig. 1A–H). Note the strong hyperkeratosis in adult mice represented by the severe thickening of the stratum corneum (Fig. 1C, G), while newborn Cx26S17F mice did not show hyperkeratosis compared to control mice (Fig. 1A, E). Marked hyperproliferation was evident in adult Cx26S17F mice while in newborn Cx26S17F mice no hyperproliferation was observed with the proliferation markers Ki67 and PCNA (Supplemental Fig. 1 and Schütz et al. [16]) indicating that hyperproliferation and hyperkeratosis developed during ageing.

To further study the abnormal lipid organisation, electron microscopic (EM) analyses on ultrathin paw sections of newborn mice were performed. They showed lipid inclusions inside the corneocytes of Cx26S17F epidermis that were not present in stratum corneum of controls (Fig. 1I and J). These inclusions are likely to represent the lipid dots seen in the Nile red staining suggesting that at least some lipids are mislocated inside the corneocytes in Cx26S17F epidermis instead of surrounding the corneocytes seen in control epidermis.

Additionally, EM analyses showed that the stratum corneum of Cx26S17F epidermis was much more compact than in controls and that aggregates of non-processed keratohyalin were still present in Cx26S17F stratum corneum (Fig. 1I and J).

3.2. Premature secretion of lipids

To characterize the epidermal lipid secretion via lamellar body release, EM analysis was performed on epidermal back skin sections of newborn mice. In control mice the secretion of lipids was observed at the stratum granulosum/stratum corneum (SC/SG) interface (Fig. 2A, white arrowheads), while in the Cx26S17F epidermis additional premature secretion was seen in the stratum granulosum (Fig. 2B, black arrowheads).

3.3. Loss of linoleoyl ω-esterified ceramides (Cer[EOS]) at the epidermal surface

In addition to the analyses of lipid distribution and secretion the ceramide composition was analysed in the epidermis by mass spectrometry. Two lipid extraction methods were used. In the first method the lipids of the intact epidermal surface of control and Cx26S17F mice were extracted by immersing newborn mice in organic solvent. In the second method the whole epidermis was lysed prior to extraction leading to recovery of ceramides from all epidermal layers.

These analyses revealed that the relative amount of the barrier-essential Cer[EOS] with fatty acid residues ranging from h30:0 to h36:0 were strongly decreased on the epidermal surface of Cx26S17F epidermis compared to control samples (Fig. 3A). In contrast, after extraction of whole epidermis, only minor differences in the relative amounts of Cer[EOS] in Cx26S17F mice were found compared to control mice (Fig. 3B). This indicates that Cer[EOS] can be synthesized but are not correctly released to the epidermal surface of Cx26S17F mice. Additionally, alterations in other ceramide classes could be observed, e.g. an increase of the relative amount of Cer[NS] (see profile of Cer[AS] and Cer[NS] in Supplemental Figs. 2 and 3).

3.4. Disturbed formation of the epidermal calcium gradient

Since the stepwise conversion of keratinocytes into corneocytes and the establishment of the epidermal barrier depend on a epidermal calcium gradient, we visualized the calcium gradient in Cx26S17F epidermis using ion-capture cytochemistry. In control epidermis the stratum granulosum contained a high number of calcium precipitates, while the stratum corneum was completely calcium free (Fig. 4A). In contrast, in the Cx26S17F epidermis large amounts of calcium intra- and extracellular of the stratum corneum as well as in the stratum corneum/stratum granulosum junction were found (Fig. 4B). This indicates that the Cx26S17F mutation leads to a disturbed calcium gradient.

4. Discussion

In this study the skin phenotype of the previously generated KID syndrome mouse model Cx26S17F was further investigated by analyzing the distribution, secretion and composition of lipids as well as the distribution of the epidermal calcium gradient.

It was previously shown that the skin phenotype of adult Cx26S27F mice (i.e. thickening and hyperkeratosis of the epidermis) is based on severe hyperproliferation [16]. Although Cx26 is expressed already during embryonic development of the skin [22], the epidermis of newborn Cx26S17F mice is not hyperproliferative (Supplemental Fig. 1). This indicates that the Cx26S17F mutation does not directly influence the proliferation rate of the epidermis during its development, but rather triggers the hyperproliferation indirectly after birth.

This trigger is likely to be the observed epidermal barrier defect which occurs already during embryonic development. It had been shown that DNA synthesis in the basal layer can be activated by barrier disruption [23]. Therefore, it is likely that the hyperproliferation in Cx26S17F mice and presumably also in KID patients is a stress response to an initial barrier defect.

The observed barrier defect can be attributed to the altered epidermal lipid properties of the Cx26S17F mice. Our results show lipid residues inside the corneocytes of the stratum corneum as well as premature secretion of lipids in stratum granulosum of Cx26S17F mice (Figs. 1 and 2). Interestingly, similar lipid residues inside corneocytes were found in a ceramide synthase 3 (CerS3) knock-out mouse line. Because of the lack of the CerS3 enzyme, the epidermis of CerS3 null mutants harbors no esterified ceramides with ultralong fatty acid residues (Cer[EOS]) [24]. Here we analyzed the ceramide composition of both the epidermis and the epidermal surface. We found that the barrier essential Cer[EOS] can be detected in samples containing whole epidermal lysates but are strongly decreased on the skin surface (Fig. 3). This indicates that Cer[EOS] can be synthesized in the epidermis, but do not correctly reach the epidermal surface, supporting the observations of premature lamellar body secretion and lipid residues inside the corneocytes.

The stepwise differentiation of the basal keratinocytes into terminally differentiated corneocytes accompanied by the establishment of the epidermal barrier is dependent on a specific amount of extra- and intracellular calcium [5]. In this study the epidermal calcium gradient was analyzed in Cx26S17F mice by ion-capture cytochemistry revealing large amounts of calcium in the normally calcium free stratum corneum (Fig. 4).

It has previously been shown that epidermal permeability and calcium barrier formation are mutually dependent on each other, as indicated by the fact that the appearance of the calcium gradient and the formation of the epidermal barrier occurs simultaneously during embryonic development [25]. In this study we have shown that in the Cx26S17F mouse line both the epidermal water barrier and the calcium gradient were disturbed. The Cx26S17F mutation may induce an imbalance of the epidermal calcium homoeostasis, either by leading to a closure of gap junction channels and hemichannels [13,14] (loss of function) or – as a recent study suggests – by hyperactivation of heteromeric hemichannels [15] (gain of function). This disturbance of epidermal calcium homeostasis could lead to an impaired lipid processing, which in turn may trigger the observed barrier impairment. It has been suggested that the fusion of the barrier lipids containing lamellar bodies is calcium dependent [25,26]. Moreover, enzymes important for barrier formation are described to be activated by calcium. For example transglutaminase 1, which catalyzes the binding of Cer[EOS] to proteins of the cornified envelope calcium dependently [27].

However, the diffusion of calcium ions into stratum corneum can be generally observed in barrier compromised skin [28]. Therefore, an alternative order of events appears to be possible in which the water barrier is disturbed prior to the changes in the calcium distribution.

One other KID syndrome mouse model has been published harboring the Cx26G45E mutation [29]. The inducible Cx26G45E mouse line develops a severe KID phenotype, e.g. a severe hyperkeratosis and scaling of the epidermis. The molecular basis leading to the observed hyperkeratosis could the same in both mouse lines. Therefore it would be interesting to analyze the lipid composition and calcium gradient in other KID mouse lines. Furthermore, it would be beneficial to analyze the epidermal barrier and surface ceramide composition in future case studies with KID patients.

Besides hyperkeratosis KID patients are prone to chronic bacterial and fungal skin infections [30–32]. It was shown that Cx26 hemichannels harboring KID mutations are activated by the pro-inflammatory mediator peptidoglycan [33]. A lowering of the epidermal barrier due to a disturbed lipid composition may enhance the susceptibility to infections in KID patients.

In summary, our study further characterizes the role of Cx26 in epidermal barrier acquisition and suggests that the skin phenotype of Cx26S17F mice may be a stress response to an initial water barrier defect. The development of epidermal hyperkeratosis may follow a similar pathway in KID patients as in Cx26S17F mice.

Supplementary Material

Refer to Web version on PubMed Central for supplementary material.

Acknowledgements

We would like to thank Brita Wilhelm and Dorothea Schünke for excellent technical assistance.

Funding The work was supported by Grants of the German Research Foundation – Germany [Wi270/30-1, Wi270/33-1 and SFB 645 project B2 to KW and Z4 to PD] and the NIH – United States of America [R21 ARO61583 and R01 AR051930 and the Research Service of the Department of Veterans Affairs and NCIRE – United States of America to TMM].

References

[1]. Richard G. Connexin disorders of the skin. Clin. Dermatol. 2005; 23:23–32. [PubMed: 15708286]

[2]. Natsuga K. Epidermal barriers. Cold Spring Harb. Perspect. Med. 2014; 4

[3]. Downing DT. Lipid and protein structures in the permeability barrier of mammalian epidermis. J. Lipid Res. 1992; 33:301–313. [PubMed: 1569381]

[4]. Rabionet M, Gorgas K, Sandhoff R. Ceramide synthesis in the epidermis. Biochim. Biophys. Acta – Mol. Cell Biol. Lipids. 2014; 1841:422–434.

[5]. Bikle DD, Xie Z, Tu C-L. Calcium regulation of keratinocyte differentiation. Expert Rev. Endocrinol. Metab. 2012; 7:461–472. [PubMed: 23144648]

[6]. Menon GK, Grayson S, Elias PM. Ionic calcium reservoirs in mammalian epidermis: ultrastructural localization by ion-capture cytochemistry. J. Invest. Dermatol. 1985; 84:508–512. [PubMed: 3998499]

[7]. Celli A, Sanchez S, Behne M, Hazlett T, Gratton E, Mauro T. The epidermal Ca(2+) gradient: measurement using the phasor representation of fluorescent lifetime imaging. celli.anna@gmail.com. Biophys. J. 2010; 98:911–921. [PubMed: 20197045]

[8]. Adams MP, Mallet DG, Pettet GJ. Active regulation of the epidermal calcium profile. J. Theor. Biol. 2012; 301:112–121. [PubMed: 22386578]

[9]. Neijssen J, Herberts C, Drijfhout JW, Reits E, Janssen L, Neefjes J. Cross-presentation by intercellular peptide transfer through gap junctions. Nature. 2005; 434:83–88. [PubMed: 15744304]

[10]. Söhl G, Willecke K. An update on connexin genes and their nomenclature in mouse and man. Cell Commun. Adhes. 2003; 10:173–180. [PubMed: 14681012]

[11]. Laird DW. Life cycle of connexins in health and disease. Biochem. J. 2006; 394:527–543. [PubMed: 16492141]

[12]. Evans WH, De Vuyst E, Leybaert L. The gap junction cellular internet: connexin hemichannels enter the signalling limelight. Biochem. J. 2006; 397:1–14. [PubMed: 16761954]

[13]. Richard G, Rouan F, Willoughby CE, Brown N, Chung P, Ryynänen M, et al. Missense mutations in GJB2 encoding connexin-26 cause the ectodermal dysplasia keratitis–ichthyosis–deafness syndrome. Am. J. Hum. Genet. 2002; 70:1341–1348. [PubMed: 11912510]

[14]. Lee JR, Derosa AM, White TW. Connexin mutations causing skin disease and deafness increase hemichannel activity and cell death when expressed in Xenopus oocytes. J. Invest. Dermatol. 2009; 129:870–878. [PubMed: 18987669]

[15]. García IE, Maripillán J, Jara O, Ceriani R, Palacios-Muñoz A, Ramachandran J, et al. Keratitis–ichthyosis–deafness syndrome-associated Cx26 mutants produce non-functional gap junctions but hyperactive hemichannels when co-expressed with wild type Cx43. J. Invest. Dermatol. 2015; 135:1338–1340. [PubMed: 25625422]

[16]. Schütz M, Auth T, Gehrt A, Bosen F, Körber I, Strenzke N, et al. The connexin 26 S17F mouse mutant represents a model for the human hereditary keratitis–ichthyosis–deafness syndrome. Hum. Mol. Genet. 2011; 20:28–39. [PubMed: 20926451]

[17]. Ilic D, Mao-Qiang M, Crumrine D, Dolganov G, Larocque N, Xu P, et al. Focal adhesion kinase controls pH-dependent epidermal barrier homeostasis by regulating actin-directed Na^+/H^+ exchanger 1 plasma membrane localization. Am. J. Pathol. 2007; 170:2055–2067. [PubMed: 17525272]

[18]. Farwanah H, Wohlrab J, Neubert RHH, Raith K. Profiling of human stratum corneum ceramides by means of normal phase LC/APCI–MS. Anal. Bioanal. Chem. 2005; 383:632–637. [PubMed: 16184366]

[19]. Welti R, Li W, Li M, Sang Y, Biesiada H, Zhou H-E, et al. Profiling membrane lipids in plant stress responses. Role of phospholipase D alpha in freezing-induced lipid changes in Arabidopsis. J. Biol. Chem. 2002; 277:31994–32002. [PubMed: 12077151]

[20]. Wewer V, Dombrink I, vom Dorp K, Dörmann P. Quantification of sterol lipids in plants by quadrupole time-of-flight mass spectrometry. J. Lipid Res. 2011; 52:1039–1054. [PubMed: 21382968]

[21]. Laemmli UK. Cleavage of structural proteins during the assembly of the head of bacteriophage T4. Nature. 1970; 227:680–685. [PubMed: 5432063]

[22]. Risek B, Klier FG, Gilula NB. Developmental regulation and structural organization of connexins in epidermal gap junctions. Dev. Biol. 1994; 164:183–196. [PubMed: 8026622]

[23]. Proksch E, Feingold KR, Man MQ, Elias PM. Barrier function regulates epidermal DNA synthesis. J. Clin. Invest. 1991; 87:1668–1673. [PubMed: 2022737]

[24]. Jennemann R, Rabionet M, Gorgas K, Epstein S, Dalpke A, Rothermel U, et al. Loss of ceramide synthase 3 causes lethal skin barrier disruption. Hum. Mol. Genet. 2012; 21:586–608. [PubMed: 22038835]

[25]. Elias PM, Nau P, Hanley K, Cullander C, Crumrine D, Bench G, et al. Formation of the epidermal calcium gradient coincides with key milestones of barrier ontogenesis in the rodent. J. Invest. Dermatol. 1998; 110:399–404. [PubMed: 9540982]

[26]. Menon GK, Price LF, Bommannan B, Elias PM, Feingold KR. Selective obliteration of the epidermal calcium gradient leads to enhanced lamellar body secretion. J. Invest. Dermatol. 1994; 102:789–795. [PubMed: 8176264]

[27]. Hitomi K. Transglutaminases in skin epidermis. Eur. J. Dermatol. 2005; 15:313–319. [PubMed: 16172037]

[28]. Elias P, Ahn S, Brown B, Crumrine D, Feingold KR. Origin of the epidermal calcium gradient: regulation by barrier status and role of active vs passive mechanisms. J. Invest. Dermatol. 2002; 119:1269–1274. [PubMed: 12485427]

[29]. Mese G, Sellitto C, Li L, Wang H-Z, Valiunas V, Richard G, et al. The Cx26-G45E mutation displays increased hemichannel activity in a mouse model of the lethal form of keratitis–ichthyosis–deafness syndrome. Mol. Biol. Cell. 2011; 22:4776–4786. [PubMed: 22031297]

[30]. Kaku Y, Tanizaki H, Tanioka M, Sakabe J, Miyagawa-Hayashino A, Tokura Y, et al. Sebaceous carcinoma arising at a chronic candidiasis skin lesion of a patient with keratitis–ichthyosis–deafness (KID) syndrome. Br. J. Dermatol. 2012; 166:222–224. [PubMed: 21777204]

[31]. Kelly B, Lozano A, Altenberg G, Makishima T. Connexin 26 mutation in keratitis–ichthyosis–deafness (KID) syndrome in mother and daughter with combined conductive and sensorineural hearing loss. Int. J. Dermatol. 2008; 47:443–447. [PubMed: 18412859]

[32]. Koppelhus U, Tranebjaerg L, Esberg G, Ramsing M, Lodahl M, Rendtorff ND, et al. A novel mutation in the connexin 26 gene (GJB2) in a child with clinical and histological features of keratitis–ichthyosis–deafness (KID) syndrome. Clin. Exp. Dermatol. 2011; 36:142–148. [PubMed: 20846357]

[33]. Donnelly S, English G, de Zwart-Storm EA, Lang S, van Steensel MAM, Martin PE. Differential susceptibility of Cx26 mutations associated with epidermal dysplasias to peptidoglycan derived from Staphylococcus aureus and Staphylococcus epidermidis. Exp. Dermatol. 2012; 21:592–598. [PubMed: 22643125]

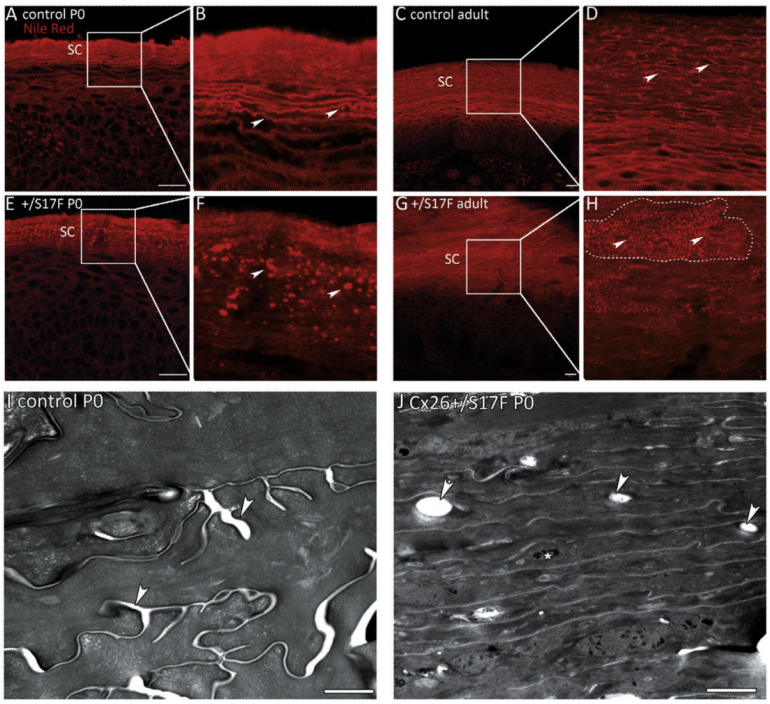

Fig. 1.

Lipid distribution in the epidermis. (A–D) Nile red stainings of paw epidermis of newborn (A, B) and adult (C, D) control mice. Examples of the evenly distributed lipid lamellae of the stratum corneum are indicated by arrows in B and D. (E–H) In newborn (E, F) and adult (G, H) Cx26S17F mice the lipids accumulate in a dot-like pattern in the stratum corneum (arrows). The stratum corneum of adult mice is strongly thickened leading to fields of “lipid-dots” (surrounded by a dashed line in H). SC: stratum corneum. Scale bars: 20 μm. (I–J) Electron micrographs of stratum corneum of paws. (I) The stratum corneum of control mice shows lipid lamellae in between the corneocytes (arrows). (J) In Cx26S17F mice the stratum corneum appears more compact than control stratum corneum. There are lipid inclusions inside the corneocytes (arrows). Additionally, aggregates of non-processed keratohyalin can be observed (asterisk). Scale bars: 1 μm.

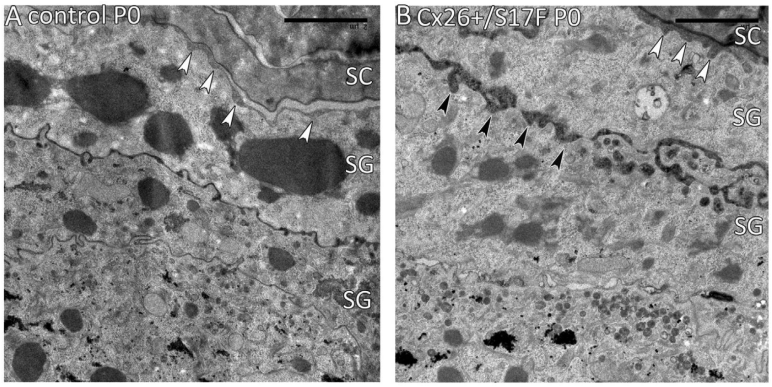

Fig. 2.

Epidermal lipid secretion. (A) Fusion of the lamellar bodies of control mice takes place at the SG/SC junction (white arrowheads). (B) In Cx26S17F mice an additional premature lipid secretion was observed in the SG (black arrowheads). SC: stratum corneum; SG: stratum granulosum. Scale bars: 2 μm.

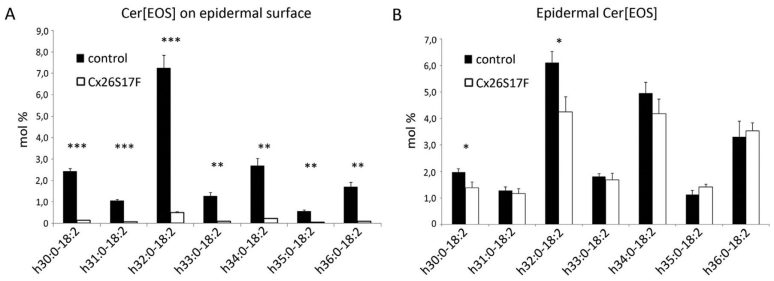

Fig. 3.

Mass spectrometric analyses of Cer[EOS]. (A) Cer[EOS] with fatty acid residues ranging from h30:0-18:2 to h36:0-18:2 on epidermal surface. The relative amount of Cer[EOS] (in mol% of all ceramides) is strongly diminished on the epidermal surface of Cx26S17F mice. n = 3. (B) Cer[EOS] composition (mol% of all ceramides) in lipid extracts from whole epidermis. Relative amounts of Cer[EOS] are only slightly decreased when extracted from all epidermal layers. n = 4. Cer: ceramide; E: esterified with linoleic acid; O: ω-hydroxylated fatty acid; S: sphingosine long chain base.

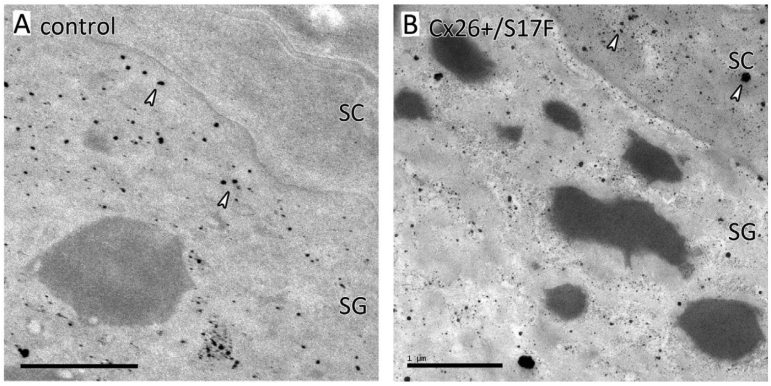

Fig. 4.

Ioncapture cytochemistry of epidermal calcium. (A) In control mice SG keratinocytes contains many calcium precipitates (arrows), while the extracellular SG/SC junction as well as the SC corneocyte are completely free of calcium. (B) In the Cx26S17F mutant large amounts of calcium are retained in the SC as well as in the extracellular SG/SC junction (arrows). SG: stratum granulosum; SC: stratum corneum; scale bar: 1 μm.